

Baryonic spin Hall effect in heavy ion collisions

Shuai Y.F. Liu¹ and Yi Yin^{1,2}

¹*Quark Matter Research Center, Institute of Modern Physics,
Chinese Academy of Sciences, Lanzhou, Gansu, 073000, China*

²*University of Chinese Academy of Sciences, Beijing, 100049, China*
(Dated: June 8, 2022)

Spin Hall effect (SHE) is the generation of spin current due to an electric field, and has been observed in a variety of materials. We investigate the perspective of detecting spin Hall current in heavy-ion collisions. While the electric field created in heavy-ion collisions has a very short lifetime, the (minus) chemical potential gradient can be viewed as an analogous electric field. Noting the longitudinal gradient of baryon chemical potential at RHIC beam energy scan (BES) energies is sizable, we predict that such “analogous baryonic electric field” will lead to spin Hall current carried by Λ ($\bar{\Lambda}$) hyperon. In addition, spin Hall current can be induced by temperature gradient, the phenomenon of which is referred to as “thermally-induced spin Hall effect” or spin Nernst effect (SNE). We propose to measure the first Fourier coefficients of local spin polarization of Λ ($\bar{\Lambda}$) with respect to azimuthal angle to probe spin Hall current, and name those observables as “directed spin flow”. By employing a thermal field theory calculation and a phenomenologically motivated freeze-out prescription for *central collisions* at a representative BES energy ($\sqrt{s} = 19.6$ GeV), we find the magnitude of the induced “directed spin flow” is of the order 10^{-3} . Furthermore, we demonstrate how to use (baryon) charge-dependent and charge-independent “directed spin flow” to discriminate spin Hall current induced by chemical potential and temperature gradient respectively.

Introduction.— The study of spin current, the flow of spin, has triggered intense research. The generation of spin current is a key concept in the field of spintronics [1], and can be employed to probe intriguing properties of quantum materials [2]. One prominent mechanism of the generation of spin current is spin Hall effect (SHE) [3], by which an electric field will induce a transverse spin current perpendicular to the direction of the electric field. SHE has been observed in a number of table-top experiments [3–5].

In this letter, we consider SHE and its analogous effect in hot and dense nuclear matter created in heavy-ion collisions. Assuming fermionic constituents of those systems are weakly coupled, one can show spin polarization distribution function of fermions (anti-fermion) in momentum space $\vec{\mathcal{P}}_+$ ($\vec{\mathcal{P}}_-$) is given by:

$$\vec{\mathcal{P}}_{\pm}^{\text{SHE}}(\mathbf{p}) = \sigma_{\pm}^H \frac{\mathbf{p}}{\varepsilon_{\mathbf{p}}} \times \vec{E}, \quad (1)$$

where \mathbf{p} denotes the spatial momentum, \hat{p} is the direction. Here, σ^H depends on temperature T and chemical potential μ of the unperturbed medium as well as the energy of fermion $\varepsilon_{\mathbf{p}} = \sqrt{\mathbf{p}^2 + m^2}$ where m is the fermion mass, and \vec{E} stands for a generic $U(1)$ charge electric field. We shall consider the simplest case when there is only one species of fermions (anti-fermions) with one unit of $U(1)$ charge throughout, although relaxing this simplification is straightforward. Based on the standard linear response theory and a thermal field theory calculation (see details below), we find

$$\sigma_{\pm}^H = \pm \frac{1}{\varepsilon_{\mathbf{p}}} \left[-\frac{\partial n_{\pm}(\varepsilon_{\mathbf{p}})}{\partial \varepsilon_{\mathbf{p}}} + \frac{n_{\pm}(\varepsilon_{\mathbf{p}})}{\varepsilon_{\mathbf{p}}} \right], \quad (2)$$

where $n_{\pm}(\varepsilon) = 1/(e^{(\varepsilon \mp \mu)/T} + 1)$ are Fermi-Dirac distribution for fermion(+) and anti-fermion (−). Previously,

Eq. (1) has been obtained in massless limit [6, 7] and in heavy mass limit $m \gg T, \mu$ [8, 9] using quantum kinetic theory (see Refs. [10, 11] for related studies). The results present here is for general μ, T, m .

In Ref. [12] where the notion of spin current is originally introduced, spin current is described by a tensor \mathcal{S}^{ij} . The first index of \mathcal{S}^{ij} indicates the direction of flow, while the second one indicates which component of the spin is flowing, i.e., $\mathcal{S}^{ij} \propto \int_{\mathbf{p}} \mathcal{P}^i(\mathbf{p}/\varepsilon_{\mathbf{p}})$. Eq. (1) then implies $\mathcal{S}^{ij} \propto \epsilon^{ijk} E_k$. In term of the terminology widely used in heavy-ion collisions community, Eq. (1) means \vec{E} will induce “local spin polarization” in the sense that while the integration of $\vec{\mathcal{P}}$ in Eq. (1) over \hat{p} vanishes for an isotropic medium, $\vec{\mathcal{P}}$ features a dipole distribution in momentum space (see Fig. 1). Regardless of the language that one chooses, Eq. (1) implies that spin flows in the plane transverse to the direction of \vec{E} .

The spin polarization induced by vorticity and magnetic field in heavy-ion collisions has attracted much experimental [13–19] and theoretical efforts [9, 20–26] (see Refs. [27–30] for reviews). Although related, the phenomenon of spin current is distinct from the spin polarization in that the former describes the motion of spin while the later does not. Therefore the observation of SHE would open a new avenue for exploring the many-body quantum effects in hot and dense nuclear/QCD matter. Unfortunately, the life-time of the electric field (of electric charge) in heavy-ion collisions is expected to be of the order 1 fm or even less. The signature of SHE induced by such electric field should be negligible. Can SHE be detected in heavy-ion collisions?

In this letter, we devise the following test for SHE in heavy-ion collisions. Our proposal relies on two observations. The first is that medium response to a (minus)

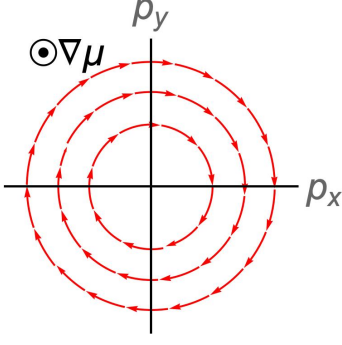


FIG. 1. (Color online) A sketch illustrating the spin polarization in momentum space induced by a chemical potential gradient $\nabla\mu$ according to Eq. (3). Here, we choose $x-y$ plane to be the plane transverse to the direction of $\nabla\mu$, and $p_{x,y}$ denote the momentum of fermions projected to x,y -directions. The arrows show the direction of spin polarization.

chemical potential gradient should be the same as that to \vec{E} . This is because chemical potential enters in the Dirac action just like the temporal component of a gauge field A_0 that couples to the fermions. One can understand this intuitively by noting the presence of charge density gradient is analogous to imposing an electric field. The second observation is that at beam energies scan (BES) energy at RHIC, the baryon density depends non-trivially on spatial rapidity, meaning the presence of sizable baryon chemical potential gradient $\nabla\mu_B$ along the longitudinal direction.

Based on the above two observations, we consider the “local spin polarization” of Λ and $\bar{\Lambda}$, $\vec{\mathcal{P}}_{\pm,\Lambda}$, at BES energies to detect SHE (see Refs. [11, 31] on the discussion of the effects of vector meson fields on hadron spin polarization). In particular, we propose the following by generalizing Eq. (1):

$$\vec{\mathcal{P}}_{\pm,\Lambda}^\mu(\mathbf{p}) = -\sigma_{\pm}^H(\varepsilon_{\mathbf{p},\Lambda}; \mu_B) \left(\frac{\mathbf{p}}{\varepsilon_{\mathbf{p}}} \right) \times \nabla\mu_B. \quad (3)$$

The spin Hall current can be induced by a temperature gradient as well. This is known as the “thermally-induced spin Hall effect” or the spin Nernst effect (SNE). The observation of SNE has been recently reported in platinum [32] and in W/CoFeB/MgO heterostructures [33]. We also find (see below for details):

$$\vec{\mathcal{P}}_{\pm}^T(\mathbf{p}) = - \left(-\frac{\partial n_{\pm}}{\partial \varepsilon} \right) \left(\frac{\mathbf{p}}{\varepsilon_{\mathbf{p}}} \right) \times \frac{\nabla T}{T}. \quad (4)$$

Previously, the relation between spin polarization and the “thermal vorticity” has been discussed in a number of references, see for example Refs. [21, 34–36] (see Ref. [37] for a review), although most of them are based on the notion of “the generalized thermal equilibrium” in the presence of vorticity. Taking such relation in the limit that the background fluid is static and homogeneous, one would obtain a similar expression $\mathcal{P} \propto \mathbf{p} \times \nabla T$ in the fluid rest frame. The effects of temperature gradient

and fluid vorticity are studied extensively in combination in order to explore spin polarization in non-central collisions [22, 23, 38]. However, the present letter is, to best of our knowledge, the first that studies the effects of temperature gradient in the context of the search for spin Hall current.

The average differential spin polarization vector of Λ and $\bar{\Lambda}$, $P_{\pm}^i(\phi_p)$, as a function of azimuthal angle ϕ_p are measured experimentally through the angular distribution of the decay daughters of $\Lambda, \bar{\Lambda}$ [16]. According to Eq. (3) (similar for Eq. (4)), the induced local spin polarization \mathcal{P} projected into the transverse plane will feature a dipole pattern, see Fig. 1. We propose to use the first Fourier coefficients of $P_{\pm}^i(\phi_p)$ ($i = x, y$) to probe the resulting spin current:

$$(a_{1,\pm}^i, v_{1,\pm}^i) \equiv \int \frac{d\phi_p}{2\pi} P_{\pm}^i \times (\sin \phi_p, \cos \phi_p). \quad (5)$$

The first Fourier harmonics of produced hadrons in heavy-ion collisions, i.e., “directed flow”, are employed to measure the flow of those hadrons. Motivated by this, we will refer $a_{1,\pm}^i, v_{1,\pm}^i$ as “directed spin flow”.

Let us discuss how to discriminate spin Hall current induced by the gradient of μ_B and T . Since the spin current of particle and anti-particle induced by the former is of the opposite sign whereas that induced by the later is the same (c.f. Eq. (2) and Eq. (4)), we expect $P_+^{i,\mu} \approx -P_-^{i,\mu}$ whereas $P_+^{i,T} \approx P_-^{i,T}$. Consequently, we shall study the following (baryon) charge-dependent and independent combination:

$$P_i^{O,S} \equiv \frac{P_{i,+} \mp P_{i,-}}{2}, \quad (6)$$

$$a_{i,1}^{S,O} \equiv \frac{a_{1,+}^i \mp a_{1,-}^i}{2}, \quad v_{i,1}^{O,S} \equiv \frac{v_{1,+}^i \mp v_{1,-}^i}{2} \quad (7)$$

where $O(S)$ correspond to $- (+)$. $a_{i,1}^O$ and $a_{i,1}^S$ are expected to be dominated by μ_B -gradient induced and T -gradient induced spin Hall current respectively.

Freezeout.— We shall benchmark the signature of the spin Hall effect. As a premier, we consider following freeze-out prescription as a proxy for \mathcal{P}^i :

$$P_{\pm}^i(\phi_p) = \frac{\int_y \int_{p_T} \int d\Sigma^\alpha p_\alpha P_{\pm,\text{lab}}^i}{2 \int_y \int_{p_T} \int d\Sigma^\alpha p_\alpha n_{\pm}(\varepsilon')} \quad (8)$$

where Σ^μ denotes the freezeout hyper-surface and the factor of 2 in the denominator accounts for 2 spin states of Λ ($\bar{\Lambda}$). A similar prescription has been used to study spin polarization induced by “thermal vorticity” [21]. Here, we boost the result in the fluid-rest frame to the lab frame. For example, for effects induced by $\nabla\mu_B$, we have

$$\mathcal{P}_{\pm,\text{lab}}^{\rho,\mu} = -\frac{1}{\varepsilon'} \varepsilon^{\rho\nu\alpha\beta} u_\nu p_\alpha \sigma_{\pm}^H(\varepsilon', \mu_B) \partial_\beta \mu_B, \quad (9)$$

where $\varepsilon' = p^\mu \cdot u_\mu$ is the single particle energy in the lab frame, and u^μ is the four flow velocity. The treatment of SNE contribution is similar. In Eq. (8), the integration

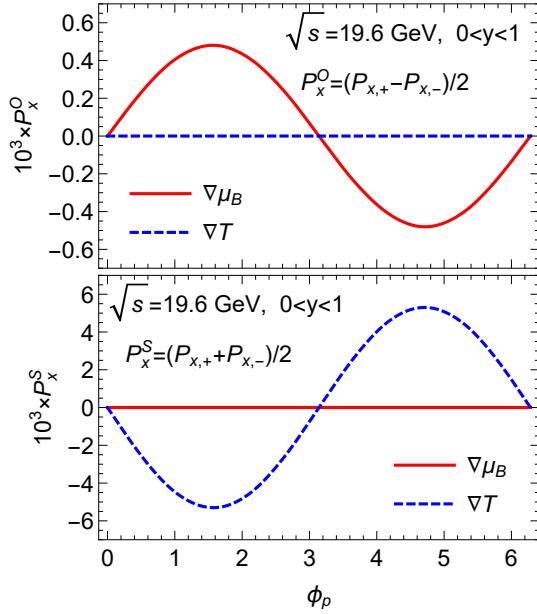


FIG. 2. (color online) We show the signature of Spin Hall current induced by baryon chemical potential gradient and temperature gradient (SNE) in $P_x^O \equiv (P_{x,+} - P_{x,-})/2$ (left panel) and $P_x^S \equiv (P_{x,+} + P_{x,-})/2$ (right panel). Here, we consider a central collision at RHIC BES energy $\sqrt{s} = 19.6$ GeV with $0 < y < 1$. The contributions from baryon chemical potential gradient and temperature gradient are shown in the red solid curve and blue dotted curve respectively. Here, $\nabla\mu_B$ is computed from Eq. (12). To evaluate SNE, we have assumed $\nabla T = -\nabla\mu$ for the present illustrative purpose.

over transverse momentum p_T and momentum rapidity y reads

$$\int_{p_T} \equiv \int_{p_T \geq p_{T,\min}} \frac{dp_T}{2\pi} p_T, \quad \int_y \equiv \int_{y_c - \Delta y}^{y_c + \Delta y} dy. \quad (10)$$

Since μ_B is symmetric in the spatial rapidity η_s , following Ref. [39], we assume that the deviation from boost invariance takes the form

$$\mu_B(\eta_s) = \mu_{B,0} + \alpha \eta_s^2, \quad (11)$$

with $\mu_{B,0}$ and α depend on the beam energy \sqrt{s} . We shall use this form for illustrative purposes, noting of course that it cannot be relied upon at large η_s .

We use $\sqrt{s} = 19.6$ GeV as an illustrative example and we focus on central collisions. We use $\alpha = 50$ MeV which is motivated by the extracted value of α at SPS energy $\sqrt{s} = 17.6$ GeV [40], and pick $\mu_{B,0} = 0.188$ GeV following Ref. [41]. While we use Eq. (11) to compute μ_B gradient in Eq. (9), we shall evaluate $\sigma_{\pm}^H(\epsilon', \mu)$, $n_{\pm}(\epsilon', \mu)$ in Eq. (9) using the parametrization of the flow profile on the freeze-out surface based on a blastwave model. Since we are considering central collisions, we will use flow profile which is boost-invariant and spherical symmetric, and further assume the freeze-out surface is isochorous at τ_f . This treatment is consistent with our formalism based on the

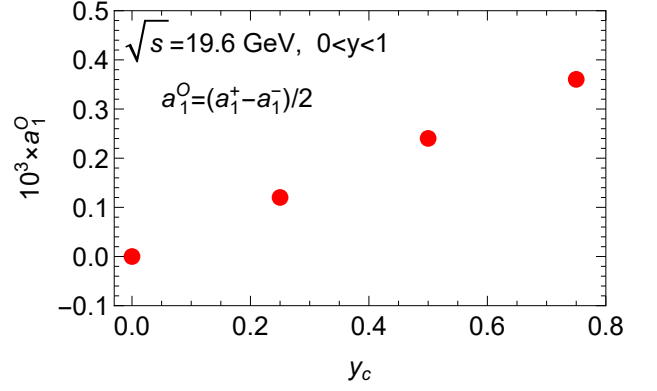


FIG. 3. We show the observable $a_{1,x}^O$ (defined in Eq. (7)), which is very sensitive to spin Hall current induced by baryon chemical potential gradient, at $\sqrt{s} = 19.6$ GeV v.s. the center of the rapidity bin y_c (see Eq. (10)).

linear response as adding non-boost invariant corrections to the evaluation of σ^H , $n_{\pm}(\epsilon', \mu)$, Σ^{μ} would lead to contribution at higher order in μ_B gradient. We parametrize radial flow as $v = 0.664(r/R)^{0.9}$, where R is the transverse radius of the fireball. Following Ref. [41], we take $T_f = 0.113$ GeV as the kinetic freeze-out temperature and use $R = 6$ fm. Evaluating $\partial_{\beta}\mu$ using Eq. (11) gives the result:

$$\partial_{\beta}\mu_B = -2\alpha \frac{\eta_s}{\tau_f} (\sinh \eta_s, 0, 0, -\cosh \eta_s). \quad (12)$$

We pick up the benchmark value $\tau_f = 10$ fm. The results with different choices of τ_f simply scales with $1/\tau_f$. For illustrative purpose, we have assumed $-\nabla T = \nabla\mu$ where the minus sign reflects the fact that temperature will decrease with increasing rapidity.

Results.— Because of the rotational symmetry in the transverse plane, $\vec{P}^z = 0$, and $\vec{P}^x(\phi_p) = \vec{P}^y(\phi_p - \pi/2)$. In particular, this indicates that $v_{1,\pm}^y = a_{1,\pm}^x$. Therefore studying $P_{x,1}^{O,S}$ and $a_{x,1}^{O,S}$ is sufficient. Note, the contribution from the gradient of the μ_B or temperature in the transverse plane will vanish in the present setup.

In Fig. 2, we plot P_x^O and P_x^S vs ϕ_p at $\sqrt{s} = 19.6$ GeV by integrating over the rapidity in the range $0 < y < 1$ and over $p_T > 0$. They both exhibit sinusoidal behavior with a period of 2π . This convincingly demonstrates that “directed spin flow” can be employed as a sensitive probe to the spin current.

Comparing Eq. (2) with Eq. (4), we expect that the ratio $|a_{1,x}^S/a_{1,x}^O| \sim \epsilon_{\Lambda}/T_f \approx 10$ assuming $|\nabla\mu| \sim |\nabla T|$, where $\epsilon_{\Lambda} \sim 1$ GeV denotes the typical energy of a Λ . This estimation is indeed confirmed by the numerical results shown in Fig. 3. Therefore, if one looks at $a_{1,\pm}^x$ individually, the result might mainly come from SNE. Despite of that, P_x^O and P_x^S are dominated by contribution from $\nabla\mu_B$ and ∇T respectively accordingly to Fig. 2. Indeed, when n_{\pm} can be approximated by Boltzmann distribution, both the numerator and the denominator of Eq. (8)

can be written as $e^{\pm\mu/T}$ times an μ -independent function. Therefore $P_+^{i,\mu} \approx -P_-^{i,\mu}$, $P_+^{i,T} \approx P_-^{i,T}$ as far as Fermi-Dirac statistic can be ignored, which is the case when $\mu_B < \varepsilon_\Lambda$.

Let us take a quick estimate on the magnitude of the signature $a_{1,x}^O$. The magnitude of $a_{1,x}^S$ is expected to be larger assuming $|\nabla T| \sim |\nabla \mu|$ as we just explained. For this purpose, let us replace $-\partial n_+(e)/\partial \varepsilon$ with $T_f^{-1} n_+(\varepsilon)$ in σ^H , and ignore the contribution from SNE. Then we have from Eqs. (8), (9), (12) that $a_{1,x}^O \sim \alpha/(\varepsilon_\Lambda T_f \tau_f)$. Plugging $\alpha = 50$ MeV, $T_f \sim 100$ MeV, $\tau_f = 10$ fm and $\varepsilon_\Lambda \sim 1$ GeV, we find $a_{1,x}^O \sim 10^{-3}$, which is consistent with results shown in Fig. 3. Although further work will be needed in order to check the present estimation quantitatively, our results provide a guidance on the feasibility of detecting baryonic SHE experimentally at BES energies.

To complement Fig. 2, we show $a_{x,1}^O$ with different choices of y_c in Fig. 3. Keeping in mind that an upgrade of the inner Time Projection Chamber (iTPC) at STAR will extend its rapidity acceptance for protons from $|y| \leq 0.5$ to $|y| \leq 0.8$, we further show results with three different values of y_c , namely $y_c = 0, 0.25, 0.5, 0.75$ with $\Delta y = 0.25$ fixed. Since the μ_B gradient becomes stronger at larger η_s according to Eq. (11), $a_{1,x}^O$ increases with a larger y_c . Therefore we anticipate that signatures of “directed spin flow” induced by $\nabla \mu_B$ will become more pronounced at forward rapidity.

While we are focus on BES energies in the present section, we point out that the signature of SNE might be detectable at top RHIC and LHC energies as well since temperature gradient is non-zero.

Conclusions and outlook.— We have made brutal simplifications in a variety of places, in particular on the density and flow profile on the freeze-out surface. We have limited ourselves to the discussion of spin current induced by longitudinal μ_B and/or T gradient, but the gradient in the transverse plane should also be present, and could lead to possible observable effects. Future studies based on the state of art hydrodynamic modeling at BES energies are desirable for quantitative prediction for the effects of spin Hall current. Here, we list a number of qualitative features that we believe to survive in such studies.

- Spin Hall current induced by the gradient of baryon chemical potential μ_B and temperature T is expected to be present in heavy-ion collisions (including central collisions) at BES energies.
- “Direct spin flow” of $\Lambda, \bar{\Lambda}$ introduced in Eq. (5) is a sensitive probe to spin Hall current.
- The combination $a_{1,i}^O, v_{1,i}^O$ and $a_{1,i}^S, v_{1,i}^S$ defined in Eq. (7) allow to discriminate the spin Hall current induced by the gradient of μ_B and T respectively. Those harmonics are of the order 10^{-3} based on the present benchmark estimation.
- $a_{1,i}^O, v_{1,i}^O$ are driven by the gradient of μ_B , and should be sensitive to beam energy and rapidity.

- $a_{1,i}^S, v_{1,i}^S$ are dominated by temperature gradient (i.e. SNE). SNE might be detectable even at top RHIC energy and LHC energies.

In addition to collisions at RHIC BES energies, SHE might be investigated at heavy-ion collisions programs at even lower beam energies, including those anticipated in the coming years, such as those at the FAIR, NICA and HIAF. Since significant baryon density gradient will be present at the forward rapidity even for top RHIC energies and LHC energies, the detector forward upgrade would be helpful for detecting SHE at those energies.

Thermal field theory calculations.— We return to details of computing Eq. (3) and Eq. (4) (SNE). Let us begin with the operator:

$$\hat{\mathcal{P}}^i(t, \mathbf{x}, \mathbf{y}) \equiv \bar{\psi}(t, \mathbf{x} + \frac{\mathbf{y}}{2}) \gamma^5 \gamma^i \psi(t, \mathbf{x} - \frac{\mathbf{y}}{2}), \quad (13)$$

where γ^5, γ^i denote the standard gamma matrices. At this point, ψ represents a generic Dirac field. According to the quantum field theory, the phase space distribution of spin polarization is given by the Wigner transform:

$$\mathcal{P}^i(t, \mathbf{x}; \mathbf{p}) = \int d^3 \mathbf{y} \langle \hat{\mathcal{P}}^i(t, \mathbf{x}, \mathbf{y}) \rangle e^{i \mathbf{p} \cdot \mathbf{y}} \quad (14)$$

with $\langle \dots \rangle$ denoting the thermal ensemble average. Here $\vec{\mathcal{P}}$ include contribution from both particles and anti-particles.

The linear response of a system disturbed slightly from equilibrium is characterized by the equilibrium expectation value of a product of two operators. To study SHE, we consider the retarded correlation function:

$$G^i(t, \mathbf{x}; \mathbf{y}) = i \langle \hat{\mathcal{P}}^i(t, \mathbf{x}; \mathbf{y}) \hat{J}^0(0, 0; 0) \rangle \theta(t), \quad (15)$$

where $\hat{J}^0 = \bar{\psi} \gamma^0 \psi$. The response of $\vec{\mathcal{P}}$ to a gauge field A_0 is given by

$$\mathcal{P}^i(q_0, \mathbf{q}; \mathbf{p}) = G^i(q_0, \mathbf{q}; \mathbf{p}) A_0(q_0, \mathbf{q}). \quad (16)$$

Here we have introduced Fourier transform with q_0, \mathbf{q} being frequency and momentum conjugate to t, \mathbf{x} respectively.

At one loop order (see Fig. 4), $G^i(\tilde{\omega}_n, \mathbf{q}; \mathbf{p})$ as a function of the Bosonic Matsubara frequency $\tilde{\omega}_n = 2n\pi T$ is given by

$$G^i = -T \sum_{\Omega_m} \text{Tr} [\gamma^i \gamma^5 S(i\nu_m + i\tilde{\omega}_n, \mathbf{p}_1) \gamma^0 S(i\nu_m, \mathbf{p}_2)], \quad (17)$$

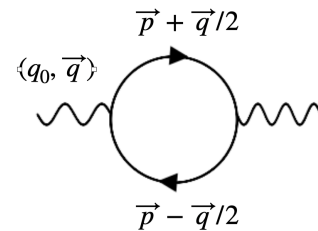


FIG. 4. One loop diagram contributing to SHE.

where $\mathbf{p}_1 = \mathbf{p} + \frac{\mathbf{q}}{2}$, $\mathbf{p}_2 = \mathbf{p} - \frac{\mathbf{q}}{2}$. Here the Euclidean propagator as function of the Fermionic Matsubara frequency $\nu_n = \pi T(2n+1) + \mu$ and momentum \mathbf{p} reads

$$S(i\nu_m, \mathbf{p}) = \sum_{s=\pm} \Lambda_s(\mathbf{p}) \Delta_s(i\nu_m, \mathbf{p}), \quad (18)$$

with $\Lambda_s(\mathbf{p}) = s\gamma^0 \varepsilon_{\mathbf{p}} - \mathbf{p} \cdot \boldsymbol{\gamma} + m$, and

$$\Delta_s(i\nu_m, \mathbf{p}) = \left(\frac{-s}{2\varepsilon_{\mathbf{p}}}\right) \frac{1}{i\nu_m - s\varepsilon_{\mathbf{p}}}. \quad (19)$$

To evaluate Eq. (17), we first take the trace:

$$\text{Tr} [\gamma^i \gamma^5 \Lambda_s(\mathbf{p}_1) \gamma^0 \Lambda_{s'}(\mathbf{p}_2)] = 4i\varepsilon^{ijm} q_j p_m, \quad (20)$$

If one were computing the response of axial current $\vec{j}_5 = \int d^3\mathbf{p}/(2\pi)^3 \vec{\mathcal{P}}$ to external disturbance by loop diagrams, one has to integrate out momentum in the loop (e.g. Ref. [42]). However, since we are interested in $\vec{\mathcal{P}}$, we only need to use the book-keeping formula to perform the summation over the Matsubara frequency:

$$\begin{aligned} & T \sum_{\Omega_m} \Delta_s(i\Omega_m + i\tilde{\omega}_n, \mathbf{p}_1) \Delta_{s'}(i\Omega_m, \mathbf{p}_2) \\ &= \sum_{ss'} \left(\frac{-ss'}{4\varepsilon_1 \varepsilon_2} \right) \left(\frac{n_s(\varepsilon_1) - n_{s'}(\varepsilon_2)}{\tilde{\omega}_m - s\varepsilon_1 + s'\varepsilon_2} \right) \end{aligned} \quad (21)$$

where $\varepsilon_{1,2} = \varepsilon_{\mathbf{p}_{1,2}}$. By substituting Eq. (20) and Eq. (21) into Eq. (17), and perform the analytic continuation, which amounts to replace $\tilde{\omega}_m$ with $q_0 + i0^+$, we obtain the desired expression

$$\begin{aligned} G^i(q_0, \mathbf{q}; \mathbf{p}) &= -\varepsilon^{iml} \frac{p^m}{\varepsilon_{\mathbf{p}}^2} i q^l \left\{ \frac{\mathbf{q} \cdot \mathbf{v}_{\mathbf{p}}}{q_0 - \mathbf{q} \cdot \mathbf{v}_{\mathbf{p}} + i0^+} \frac{\partial n_+(\varepsilon_{\mathbf{p}})}{\partial \varepsilon_{\mathbf{p}}} \right. \\ &\quad \left. - \frac{\mathbf{q} \cdot \mathbf{v}_{\mathbf{p}}}{q_0 + \mathbf{q} \cdot \mathbf{v}_{\mathbf{p}} + i0^+} \frac{\partial n_-(\varepsilon_{\mathbf{p}})}{\partial \varepsilon_{\mathbf{p}}} + \frac{n_+(\varepsilon_{\mathbf{p}}) + n_-(\varepsilon_{\mathbf{p}})}{\varepsilon_{\mathbf{p}}} \right\} \end{aligned} \quad (22)$$

Here, we have used $\varepsilon_1 - \varepsilon_2 = \mathbf{v}_{\mathbf{p}} \cdot \mathbf{q}$, $n_{\pm}(\varepsilon_1) - n_{\pm}(\varepsilon_2) = (\partial n_{\pm}(\varepsilon_{\mathbf{p}})/\partial \varepsilon_{\mathbf{p}}) \mathbf{v}_{\mathbf{p}} \cdot \mathbf{q}$ by assuming $q_0, q \ll \varepsilon_{\mathbf{p}} \sim T, \mu$. In another word, we have expanded G^i to the first non-trivial order in $q_0/\varepsilon_{\mathbf{p}}, q/\varepsilon_{\mathbf{p}}$ to obtain (22).

We now extract the induced fermion (anti-fermion) local spin polarization $\vec{\mathcal{P}}_+$ ($\vec{\mathcal{P}}_-$) from Eq. (22) and Eq. (16). We assume that \mathcal{P}_+ (\mathcal{P}_-) should depend on n_+ (n_-) and/or the derivative $\partial n_+/\partial \varepsilon_{\mathbf{p}}$ ($\partial n_-/\partial \varepsilon_{\mathbf{p}}$) only, and require $\vec{\mathcal{P}}(\mathbf{p}) = \vec{\mathcal{P}}_+(\mathbf{p}) + \vec{\mathcal{P}}_-(-\mathbf{p})$. We therefore have:

$$\mathcal{P}_+^i = g_+(q_0, \mathbf{q}; \mu) (i\varepsilon^{iml} p^m q^l A_0(q_0, \mathbf{q})), \quad (23)$$

where

$$g_+ = \frac{-1}{\varepsilon_{\mathbf{p}}^2} \left[\frac{\mathbf{q} \cdot \mathbf{v}_{\mathbf{p}}}{q_0 - \mathbf{q} \cdot \mathbf{v}_{\mathbf{p}} + i0^+} \frac{\partial n_+(\varepsilon_{\mathbf{p}})}{\partial \varepsilon_{\mathbf{p}}} + \frac{n_+(\varepsilon_{\mathbf{p}})}{\varepsilon_{\mathbf{p}}} \right] \quad (24)$$

Comparing Eq. (3) in Fourier space with Eq. (23) we then determine σ_+^H :

$$\sigma_+^H \equiv -\lim_{\mathbf{q} \rightarrow 0} \lim_{q_0 \rightarrow 0} [\varepsilon_{\mathbf{p}} g_+(q_0, \mathbf{q}; \mu)]. \quad (25)$$

A similar procedure leads to σ_-^H , and completes our derivation of Eq. (2). Note $\sigma_-^H(\varepsilon_{\mathbf{p}}; \mu) = -\sigma_+^H(\varepsilon_{\mathbf{p}}, -\mu)$

The cautious reader might worry if one could do such separation when fermion and anti-fermion are mixed with each in the presence of $A_0(q_0, \mathbf{q})$. However, since we consider fermions with energy $\varepsilon_{\mathbf{p}} \gg q, q_0$, they will interact with anti-fermions of approximately the same energy $\varepsilon_{\mathbf{p}}$, meaning the relative phase between the fermions and anti-fermions participated in such interaction is approximately $2\varepsilon_{\mathbf{p}}\Delta t$ for a given duration Δt . Therefore one should be able to integrate out fast oscillating anti-fermions in the long time limit and hence obtain distribution for fermions. A parallel conclusion can be drawn for anti-fermions. See Refs. [6, 43, 44] for explicit examples on obtaining particle/anti-particle distribution through such integrating-out procedure.

In Eq. (25), we take the static limit to obtain σ^H by assuming that typical gradient \mathbf{q} is much larger than the frequency q_0 and the collision rate. As usual, the order of limit matters. Taking the limit with an opposite order corresponds to studying the real-time dynamics of SHE. We leave this for future study

Turning to SNE, we consider gravigauge field $g^{00} = -1 + \log T$. Defining the retarded Green function

$$G^{i,0\mu}(t, \mathbf{x}) = i\langle \mathcal{P}^i(t, \mathbf{x}) T^{0\mu}(0, 0) \rangle \theta(t), \quad (26)$$

we have:

$$\mathcal{P}_{\text{SNE}}^i(q_0, \mathbf{q}; \mathbf{p}) = G^{i,00}(q_0, \mathbf{q}; \mathbf{p}) \log [T(q_0, \mathbf{q})]. \quad (27)$$

At one loop order the expression for $G^{i,00}$ is given by replacing γ^0 in Eq. (17) with $\gamma^0 i\nu_m$. Hence the evaluation of $G^{i,00}$ then becomes a trivial extension of the calculation of G^i . We find

$$\begin{aligned} G^{i,00}(q_0, \mathbf{q}; \mathbf{p}) &= -i\varepsilon^{ilm} p^l q^m \left\{ \frac{\mathbf{q} \cdot \mathbf{v}_{\mathbf{p}}}{q_0 - \mathbf{q} \cdot \mathbf{v}_{\mathbf{p}} + i0^+} \frac{\partial n_+(\varepsilon_{\mathbf{p}})}{\partial \varepsilon_{\mathbf{p}}} \right. \\ &\quad \left. + \frac{\mathbf{q} \cdot \mathbf{v}_{\mathbf{p}}}{q_0 + \mathbf{q} \cdot \mathbf{v}_{\mathbf{p}} + i0^+} \frac{\partial n_-(\varepsilon_{\mathbf{p}})}{\partial \varepsilon_{\mathbf{p}}} \right\}, \end{aligned} \quad (28)$$

Substituting Eq. (28) into Eq. (27) and taking the static limit, we arrive at Eq. (4).

A similar step determines $\vec{\mathcal{P}}$ induced by the gradient of flow velocity. The result will be reported in upcoming work [45].

Acknowledgments.— We are grateful to Koichi Hattori, Xu-Guang Huang, Shu Lin, Hao Qiu, Chun Shen, Pu Shi, Subhash Singha, Xin-Li Sheng, Shusu Shi, Shuzhe Shi, Qun Wang, Naoki Yamamoto, Ho-Ung Yee, Jie Zhao for helpful conversations. We in particular thank Longgang Pang for drawing us the attention to Ref. [38], which motivates this letter. This work was supported by the Strategic Priority Research Program of Chinese Academy of Sciences, Grant No. XDB34000000.

-
- [1] I. Žutić and H. Dery, *Nature Materials* **10**, 647 (2011).
- [2] W. Han, S. Maekawa, and X.-C. Xie, *Nature Materials* **19**, 1 (2019).
- [3] J. Sinova, S. O. Valenzuela, J. Wunderlich, C. H. Back, and T. Jungwirth, *Rev. Mod. Phys.* **87**, 1213 (2015).
- [4] C. L. Kane and E. J. Mele, *Phys. Rev. Lett.* **95**, 226801 (2005).
- [5] J. Wunderlich, B. Kaestner, J. Sinova, and T. Jungwirth, *Phys. Rev. Lett.* **94**, 047204 (2005).
- [6] D. T. Son and N. Yamamoto, *Phys. Rev. D* **87**, 085016 (2013), arXiv:1210.8158 [hep-th].
- [7] Y. Hidaka, S. Pu, and D.-L. Yang, *Phys. Rev. D* **95**, 091901 (2017), arXiv:1612.04630 [hep-th].
- [8] K. Hattori, Y. Hidaka, and D.-L. Yang, *Phys. Rev. D* **100**, 096011 (2019), arXiv:1903.01653 [hep-ph].
- [9] R.-h. Fang, L.-g. Pang, Q. Wang, and X.-n. Wang, *Phys. Rev. C* **94**, 024904 (2016), arXiv:1604.04036 [nucl-th].
- [10] S. Pu, S.-Y. Wu, and D.-L. Yang, *Phys. Rev. D* **91**, 025011 (2015), arXiv:1407.3168 [hep-th].
- [11] X.-L. Sheng, L. Oliva, and Q. Wang, *Phys. Rev. D* **101**, 096005 (2020), arXiv:1910.13684 [nucl-th].
- [12] M. I. D'Yakonov and V. I. Perel', *Soviet Journal of Experimental and Theoretical Physics Letters* **13**, 467 (1971).
- [13] L. Adamczyk et al. (STAR), *Nature* **548**, 62 (2017).
- [14] T. Niida (STAR), *Nucl. Phys. A* **982**, 511 (2019).
- [15] J. Adam et al. (STAR), *Phys. Rev. C* **98**, 014910 (2018), arXiv:1805.04400 [nucl-ex].
- [16] J. Adam et al. (STAR), *Phys. Rev. Lett.* **123**, 132301 (2019), arXiv:1905.11917 [nucl-ex].
- [17] S. Acharya et al. (ALICE), *Phys. Rev. C* **101**, 044611 (2020), arXiv:1909.01281 [nucl-ex].
- [18] S. Acharya et al. (ALICE), (2019), arXiv:1910.14408 [nucl-ex].
- [19] C. Zhou, *Nucl. Phys. A* **982**, 559 (2019).
- [20] J.-H. Gao, Z.-T. Liang, S. Pu, Q. Wang, and X.-N. Wang, *Phys. Rev. Lett.* **109**, 232301 (2012).
- [21] F. Becattini, V. Chandra, L. Del Zanna, and E. Grossi, *Annals Phys.* **338**, 32 (2013), arXiv:1303.3431 [nucl-th].
- [22] L.-G. Pang, H. Petersen, Q. Wang, and X.-N. Wang, *Phys. Rev. Lett.* **117**, 192301 (2016).
- [23] F. Becattini and I. Karpenko, *Phys. Rev. Lett.* **120**, 012302 (2018).
- [24] W. Florkowski, A. Kumar, R. Ryblewski, and R. Singh, *Phys. Rev. C* **99**, 044910 (2019).
- [25] S. Y. Liu, Y. Sun, and C. M. Ko, (2019), arXiv:1910.06774 [nucl-th].
- [26] N. Weickgenannt, E. Speranza, X.-l. Sheng, Q. Wang, and D. H. Rischke, (2020), arXiv:2005.01506 [hep-ph].
- [27] D. Kharzeev, J. Liao, S. Voloshin, and G. Wang, *Prog. Part. Nucl. Phys.* **88**, 1 (2016), arXiv:1511.04050 [hep-ph].
- [28] A. Bzdak, S. Esumi, V. Koch, J. Liao, M. Stephanov, and N. Xu, *Phys. Rept.* **853**, 1 (2020), arXiv:1906.00936 [nucl-th].
- [29] F. Becattini and M. A. Lisa, (2020), 10.1146/annurev-nucl-021920-095245, arXiv:2003.03640 [nucl-ex].
- [30] J.-H. Gao, G.-L. Ma, S. Pu, and Q. Wang, (2020), arXiv:2005.10432 [hep-ph].
- [31] L. Csernai, J. Kapusta, and T. Welle, *Phys. Rev. C* **99**, 021901 (2019), arXiv:1807.11521 [nucl-th].
- [32] S. Meyer, Y.-T. Chen, S. Wimmer, M. Althammer, S. Geprgs, H. Huebl, D. KAdderitzsch, H. Ebert, G. Bauer, R. Gross, and S. Goennenwein, *Nature Materials* **16** (2016), 10.1038/nmat4964.
- [33] P. Sheng, Y. Sakuraba, Y.-C. Lau, S. Takahashi, S. Mitani, and M. Hayashi, *Science Advances* **3** (2017), 10.1126/sciadv.1701503, <https://advances.sciencemag.org/content/3/11/e1701503.full.pdf>.
- [34] F. Becattini and F. Piccinini, *Annals Phys.* **323**, 2452 (2008), arXiv:0710.5694 [nucl-th].
- [35] F. Becattini, F. Piccinini, and J. Rizzo, *Phys. Rev. C* **77**, 024906 (2008), arXiv:0711.1253 [nucl-th].
- [36] X.-L. Sheng, Q. Wang, and X.-G. Huang, (2020), arXiv:2005.00204 [hep-ph].
- [37] F. Becattini (2020) arXiv:2004.04050 [hep-th].
- [38] H.-Z. Wu, L.-G. Pang, X.-G. Huang, and Q. Wang, *Phys. Rev. Research* **1**, 033058 (2019), arXiv:1906.09385 [nucl-th].
- [39] J. Brewer, S. Mukherjee, K. Rajagopal, and Y. Yin, *Phys. Rev. C* **98**, 061901 (2018), arXiv:1804.10215 [hep-ph].
- [40] F. Becattini, J. Cleymans, and J. Strumpf, *PoS CPOD07*, 012 (2007), arXiv:0709.2599 [hep-ph].
- [41] L. Adamczyk et al. (STAR), *Phys. Rev. C* **96**, 044904 (2017), arXiv:1701.07065 [nucl-ex].
- [42] S. Lin and L. Yang, *Phys. Rev. D* **98**, 114022 (2018), arXiv:1810.02979 [nucl-th].
- [43] C. Manuel and J. M. Torres-Rincon, *Phys. Rev. D* **90**, 076007 (2014), arXiv:1404.6409 [hep-ph].
- [44] C. Manuel, J. Soto, and S. Stetina, *Phys. Rev. D* **94**, 025017 (2016), [Erratum: *Phys. Rev. D* **96**, 129901 (2017)], arXiv:1603.05514 [hep-ph].
- [45] S. Liu, L. Pang, and Y. Yin, in preparation (2020).